Resonance Raman Spectrum of *all-trans*-Spheroidene. DFT Analysis and Isotope Labeling

A. M. Dokter,[†] M. C. van Hemert,[‡] C. M. In 't Velt,[†] K. van der Hoef,[‡] J. Lugtenburg,[‡] H. A. Frank,[§] and E. J. J. Groenen*[,†]

Department of Molecular Physics, Huygens Laboratory, Leiden University, P.O. Box 9504, 2300 RA Leiden, The Netherlands, Leiden Institute of Chemistry, Gorlaeus Laboratories, Leiden University, P.O. Box 9502, 2300 RA Leiden, The Netherlands, and Department of Chemistry, University of Connecticut, Storrs, Connecticut

Received: May 23, 2002; In Final Form: August 19, 2002

Density-functional theory has been applied to analyze the resonance Raman spectrum of the carotenoid *all-trans*-spheroidene. Besides natural-abundance spheroidene, 19 ^{2}H- or ^{13}C-containing isotopomers have been taken into consideration. Calculated frequencies are found to be in excellent agreement with experiment. In particular, the observed variation of vibrational frequencies with isotopic composition is nicely reproduced, which proves the assignments. A simple estimate of the resonance Raman intensities correctly predicts which vibrational transitions are resonance enhanced. Density-functional theory is well suited to describe the normal-mode structure of a molecule as large as a carotenoid.

Introduction

The use of density-functional theory (DFT) to describe the vibrations of organic molecules is well established. Calculations on molecules of moderate size have shown that the combination of the 6-31G* basis set and the B3LYP exchange-correlation functional presents a suitable compromise between accuracy and applicability.[1−3] Recently, such calculations were extended to larger molecules such as long polyenes,[4] *all-trans*-retinal,[5] and fullerenes.[6] For these larger molecules the observed correlation between experimental and calculated vibrational frequencies is as such less convincing in regard to the quality of the theoretical analysis, because the increase in the number of modes in a limited frequency range entails an assignment problem. A combined experimental and theoretical study of the effects of isotopic substitutions would represent a critical test of the accuracy of the DFT procedure. The *all-trans*-spheroidene molecule presents a challenge in this respect.

Spheroidene is the carotenoid bound to the reaction center of anaerobically grown *Rhodobacter sphaeroides* wild-type strain 2.4.1.[7] Its 15,15′-cis configuration and nonplanarity are amply documented on the basis of resonance Raman[8] and NMR[9] spectroscopy. Precise structural information can in principle be obtained from single-crystal X-ray diffraction studies but as yet the quality of the electron density maps for reaction centers of purple bacteria is insufficient to derive a detailed structure of the carotenoids.[10] This even applies to recent diffraction data up to 2.1 Å resolution for a mutant *Rh. sphaeroides* reaction center, which contains spheroidenone.[11] In this case the data were found to be consistent with a 15,15′-cis configuration of the carotenoid.

Several years ago, we embarked upon a project that aims at the determination of the structure of the carotenoid spheroidene in the reaction center from resonance Raman spectroscopy. To this end we (i) synthesize a variety of spheroidenes ^{2}H or ^{13}C labeled at specific positions, (ii) reconstitute these spheroidenes into the reaction-center complex of the carotenoidless mutant *Rb. sphaeroides* R26, and (iii) investigate the resonance Raman spectra of the labeled spheroidenes in an organic solvent and of the reconstituted reaction centers. We have reported resonance Raman data for both ^{13}C- and ^{2}H-labeled spheroidenes[12,13] and qualitatively discussed the spectra in the 900−1600 cm^{-1} region. A quantitative description requires a full analysis of the normal-mode structure, which is nontrivial for a molecule of this size. In the present paper we demonstrate, as a first step, the feasibility of such an analysis for the *all-trans*-spheroidene.

We report on the calculation by DFT of the resonance Raman spectrum of *all-trans*-spheroidene, both of natural-abundance (NA) and of 19 ^{2}H- or ^{13}C-labeled isotopomers. Comparison of the calculated isotope-induced spectral changes with those observed experimentally reveals that the calculations almost quantitatively reproduce the experimental data, which underscores the accuracy of the DFT approach. A complete description of the normal-mode structure of *all-trans*-spheroidene has been obtained.

Method

The molecular structure of *all-trans*-spheroidene is represented in Figure 1. The transitions that show up in the resonance Raman spectra derive from the vibrational modes in the conjugated part of the molecule. In the calculations we therefore considered a truncated molecule corresponding to the C_3 to $C_{9'}$ part of spheroidene (cf. Figure 1), terminated by methyl groups whose carbons we have assigned masses of 86 (equivalent to $C_5H_{11}O$) and 148 (equivalent to $C_{11}H_{19}$) atomic units.

The calculation consists of four steps.

(i) Geometry optimization. DFT calculations were performed using the Gaussian 98, Rev. A.5. package,[14] on a 15 node IBM SP2 computer. The hybrid B3LYP functional was used in combination with a 6-31G* basis set. As a starting geometry the AM1-optimized structure calculated by Connors et al.[15] was

* Corresponding author. Phone: +31-71-5275914. Fax: +31-71-5275819. E-mail: mat@molphys.leidenuniv.nl.
† Department of Molecular Physics, Huygens Laboratory, Leiden University.
‡ Leiden Institute of Chemistry, Gorlaeus Laboratories, Leiden University.
§ Department of Chemistry, University of Connecticut.

10.1021/jp026164e CCC: $22.00
Published on Web 09/19/2002

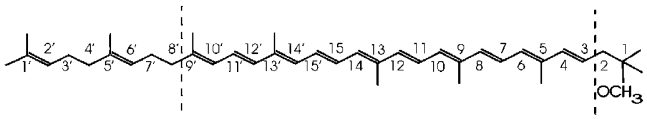

Figure 1. Molecular structure of *all-trans*-spheroidene. The conjugated part considered in the calculations is indicated.

used. For the geometry optimization the Berny algorithm was employed and an ultrafine integration grid for the numerical calculation of the two-electron integrals. The optimization was performed in redundant internal coordinates. This (time-consuming) part of the calculation has only to be performed for one of the isotopomers.

(ii) Calculation of the Hessian in Cartesian coordinates and subsequent transformation to mass-weighted coordinates.

(iii) Calculation of normal modes and frequencies. The Wilson GF formalism has been used. Equivalent results have been obtained using the Freq keyword in Gaussian, but to calculate the resonance Raman intensities, we needed the **A**-matrix that describes the normal coordinates in terms of the internal coordinates. This matrix is not provided by Gaussian and therefore we have used a home-written program based on the Wilson GF formalism. The frequencies have been uniformly scaled by a factor of 0.963, a value established previously on the basis of calculations on 31 small and medium-sized organic molecules.[1]

(iv) Estimation of the resonance Raman intensities. The intensity I_α of normal mode α was calculated according to

$$I_\alpha \sim \nu_\alpha \left(\sum_i A_{\alpha i}\delta_i\right)^2 \qquad (1)$$

where ν_α represents the frequency of mode α, **A** is the transformation matrix of internal into normal coordinates, and δ_i the displacement in internal coordinate *i* accompanying the electronic transition resonant with the laser excitation frequency. Equation 1 is based on the Albrecht **A**-term,[16] which is known to be dominant for a conjugated molecule in the case of resonance with a strong electronic transition.[17] Assuming harmonic potential energy surfaces in both the ground and excited states, and the same normal coordinates and frequencies in both states, it has been shown that the intensity becomes proportional to the square of the displacement between the ground- and excited-state equilibrium geometries.[18]

To be able to use eq 1, a suitable set of δ_i's is needed. The Raman spectra are obtained with excitation at 496.5 nm,[12,13] in resonance with the strongly allowed $\pi\pi^*$ excitation. A lengthening of the carbon−carbon double bonds and a shortening of the carbon−carbon single bonds accompany such an excitation.[19] Only those normal modes that contain C−C or C═C stretch character acquire resonance Raman intensity. We have determined a set of relative values of δ_i for these bonds iteratively (using the Igor Pro version 4.0.1.0 software package) by fitting the intensities calculated according to eq 1 to the intensities measured for 565 modes of 8 isotopomers (NA, 11-^{13}C, 13-^{13}C, 15-^{2}H, 15′-^{2}H, 15′-^{13}C, 14′-^{13}C, and 15,15′-^{2}H$_2$ spheroidene). These 8 isotopomers have been chosen more or less arbitrarily out of the total set of 20, taking care that not too many isotopomers were included that show rather similar spectra.

Note that whereas natural-abundance spheroidene contains 1.1% ^{13}C and 0.015% ^{2}H, the calculation on "natural-abundance" spheroidene refers to a molecule consisting of only ^{12}C and ^{1}H.

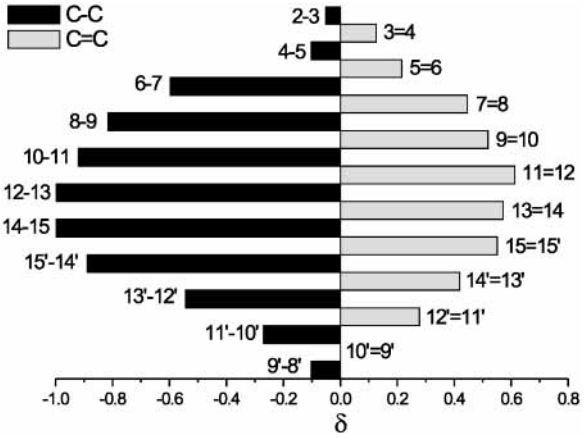

Figure 2. Changes δ (in relative units) of the length of the carbon−carbon bonds of *all-trans*-spheroidene upon optical excitation at 496.5 nm. The numbering of the carbon atoms refers to Figure 1.

TABLE 1: Carbon−Carbon Bond Lengths (pm) in the Optimized Geometry of the C_3 to $C_{9'}$ Part of *all-trans*-Spheroidene

C═C bonds	length (pm)	C−C bonds	length (pm)
3═4	134.72	4−5	145.72
5═6	136.66	6−7	143.67
7═8	136.37	8−9	144.42
9═10	137.25	10−11	143.17
11═12	136.65	12−13	144.13
13═14	137.43	14−15	142.88
15═15′	136.82	15′−14′	143.01
14′═13′	137.21	13′−12′	144.66
12′═11′	136.04	11′−10′	144.43
10′═9′	135.43		

Results

The lengths of the carbon−carbon bonds in the optimized geometry are represented in Table 1 (the full structure is available as supporting material, Table 1S). The estimated relative change of these lengths upon excitation is represented in Figure 2. The bond-length changes δ_i are maximal around the center of the conjugated chain (not the center of the molecule) and gradually decrease toward the ends of the conjugated chain.

As reference points for our calculations we have at our disposal the resonance Raman spectra of NA and isotopically labeled spheroidenes in petroleum ether: 15′-^{13}C and 14′-^{13}C (ref 12); 14-^{2}H, 15-^{2}H, 15′-^{2}H, 14′-^{2}H, 14,15′-^{2}H$_2$, and 15,15′-^{2}H$_2$ (ref 13); 8-^{13}C, 10-^{13}C, 11-^{13}C, 13-^{13}C, 13,14-^{13}C$_2$, 10-^{2}H, 11-^{2}H, 12-^{2}H, 11′-^{2}H, 10,12-^{2}H$_2$, and 12,14-^{2}H$_2$ (ref 20). As examples of the experimental spectra, those for NA and 15,-15′-^{2}H$_2$ spheroidene are shown in Figure 3. The Raman intensity is largely concentrated in three regions, around 1000 cm^{-1}, between 1100 and 1300 cm^{-1}, and between 1500 and 1550 cm^{-1}, whereas for the ^{2}H-labeled spheroidenes intensity is present between 920 and 970 cm^{-1} as well.

The calculated resonance Raman spectra for NA spheroidene and the 15,15′-^{2}H$_2$ isotopomer are represented by stick spectra in Figure 3, where the length of the sticks is proportional to the resonance Raman intensity calculated according to eq 1. Table 2 lists for NA spheroidene the calculated frequencies, the intensities, and the compositions of the normal modes that carry resonance Raman intensity. A table with all calculated normal-mode frequencies and resonance Raman intensities for all isotopomers is available as supporting material (Table 2S). The correlation between calculated and experimental frequencies between 950 and 1600 cm^{-1} for NA spheroidene is represented

TABLE 2: Calculated Frequencies, Resonance Raman Intensities (Relative to That of the 1523 cm^{-1} Mode), and Composition of the Normal Modes of Natural-Abundance *all-trans*-Spheroidene[a]

frequency (cm^{-1})	intensity (%)	mode composition
996	7	
1011	1	
1013	1	
1157	6	− 0.15(6═7) − 0.11(10═11) + 0.10(14═15) − 0.12(15′═14′) + 0.11(11′═10′) − 0.19(7H) + 0.12(12H) + 0.20(12′H) + 0.12(11′H) + 0.24(10′H)
1162	35	+ 0.15(10═11) + 0.15(14═15) + 0.11(15′═14′) + 0.16(11′═10′) + 0.14(11H) + 0.16(15H) − 0.10(15′H) + 0.14(12′H) + 0.24(10′H)
1183	2	
1191	8	+ 0.14(4═5) + 0.10(8═9) − 0.16(4H) − 0.29(6H) − 0.23(7H) − 0.35(8H) − 0.24(10H) − 0.18(11H) − 0.20(12H) − 0.10(14H)
1195	3	
1205	2	
1216	2	
1268	2	
1291	2	
1313	3	
1360	2	
1401	1	
1461	4	
1463	7	− 0.09(13═14) − 0.08(14′═13′) + 0.15(14H) − 0.14(14′H)
1523	100	− 0.09(7═8) − 0.12(9═10) − 0.13(11═12) − 0.19(13═14) − 0.08(15═15′) − 0.14(14′═13′) + 0.09(10−11) + 0.09(12−13) + 0.10(14−15) − 0.16(7H) + 0.17(8H) + 0.16(10H) − 0.27(11H) + 0.24(12H) + 0.22(14H) − 0.24(15H) + 0.16(15′H) − 0.21(14′H) − 0.17(12′H)
1530	8	+ 0.09(7═8) − 0.09(9═10) + 0.17(11═12) − 0.13(13═14) + 0.21(15═15′) − 0.12(14′═13′) + 0.08(12′═11′) + 0.14(7H) + 0.23(11H) − 0.21(12H) + 0.24(15H) − 0.28(15′H) − 0.15(11′H)
1561	2	

[a] Only the modes for which the calculated resonance Raman intensity amounts to at least 1% of that of the 1523 cm^{-1} mode have been tabulated. The composition of a normal coordinate (α) is given in terms of internal coordinates (i), where the coefficients equal the matrix elements $A_{\alpha i}$ (see eq 1). The coordinate A−B (A═B) denotes the internal stretch coordinate related to the atoms C_A and C_B. The coordinate nH denotes the internal coordinate defined by the angle H_n−C_n−C_m, where C_m is the carbon atom in the conjugated chain to the right of C_n (see Figure 1). Different types of internal motion (e.g., C═C stretch, C−C stretch, H-bend) do not contribute to the same extent to the total vibrational energy, because of the different values of the force constants associated with each internal coordinate. Internal coordinates corresponding to carbon−carbon stretch vibrations with coefficients smaller than 0.07 and internal coordinates corresponding to bend vibrations with coefficients smaller than 0.1 have not been listed.

in Figure 4. This graph is based on the assumption that an experimental frequency is assigned to the nearest calculated frequency for which the calculation predicts appreciable intensity.

The variation of the Raman frequencies of the most intense bands in the fingerprint region and in the C═C stretch region as a function of isotopic composition is represented in Figure 5, both for the experimental spectra and for the calculated spectra. In the 1150−1170 cm^{-1} region mostly two bands of appreciable intensity are calculated and observed, and in those cases the intensity-weighted average frequency is taken in Figure 5.

Discussion

Based upon a DFT calculation on the conjugated part of the *all-trans*-spheroidene molecule, a detailed interpretation has been obtained of the resonance Raman spectrum of this carotenoid in petroleum ether. Previously[13] we have discussed qualitatively the spectra available at that time on the basis of the analogy with related polyenes, in particular retinal and β-carotene for which descriptions based on normal-coordinate analyses were available.[21,22] Meanwhile resonance Raman spectra have been obtained of many more isotopomers, and DFT has been successfully applied to vibrational calculations on small and medium-sized organic molecules.[1−6] Our present results show that the former qualitative description was too simple in many respects.

Density-functional theory allows an essentially complete analysis of the resonance Raman spectrum of *all-trans*-spheroidene. The calculations for the isotopically labeled spheroidenes unequivocally show that also for a molecule of this size the combination of the 6-31G* basis set and the B3LYP exchange-correlation functional provides an accurate description of the vibrational modes. When considering only natural-abundance *all-trans*-spheroidene, the observed correlation of experimental and calculated frequencies (cf. Figure 4) would not be convincing, because of the uncertainty with regard to the underlying assignments. The data for the ^{2}H and ^{13}C isotopomers preclude misassignments, and, as seen in Figure 5, spectral changes observed upon isotopic substitution are largely reproduced in the DFT calculations. To discuss the calculations in detail, we consider successively various spectral regions.

1500−1600 cm^{-1} Region. Vibrational modes in this region are mainly composed of C═C stretch vibrations. For most isotopomers, the resonance Raman intensity is largely concentrated in one band which in good approximation can be considered as an in-phase combination of C═C stretches in the C_7 to $C_{13'}$ part of spheroidene. This is illustrated in Figure 6a for the mode of NA spheroidene calculated and observed at 1523 cm^{-1}, whose composition is given in Table 2. The intensity is essentially determined by the weight of the C═C stretches in the central part of the conjugated chain where the change (δ) of the carbon−carbon bond lengths upon excitation is largest (cf. Figure 2). As long as the normal-mode structure does not change significantly, the introduction of heavier atoms (i.e., ^{2}H or ^{13}C) will lead to lower vibrational frequencies. For many isotopomers a second band in this region acquires intensity (cf.

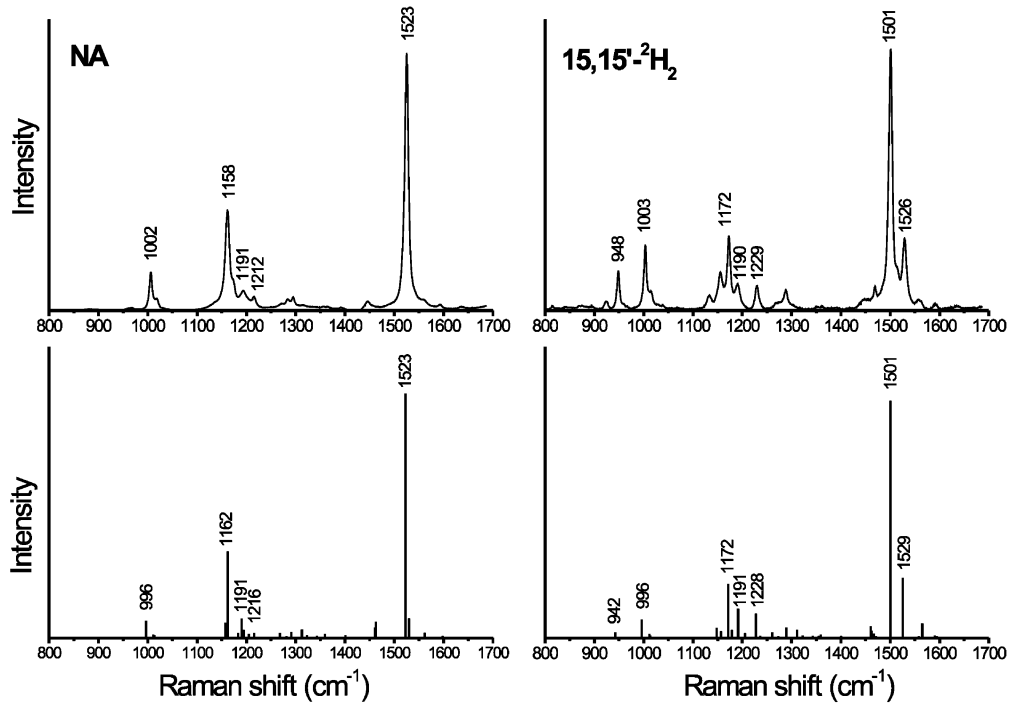

Figure 3. Experimental (top) and calculated (bottom) resonance Raman spectra of natural-abundance (left) and 15,15′-$^2H_2$ (right) *all-trans*-spheroidene. The shoulder in the experimental spectrum of the 15,15′-$^2H_2$ isotopomer at 1514 cm^{-1} (not reproduced in the calculation) most probably derives from a singly ^{2}H-substituted impurity in the sample (the most intense bands for 15-^{2}H and 15′-^{2}H *all-trans*-spheroidene occur at 1513 and 1514 cm^{-1}, respectively).

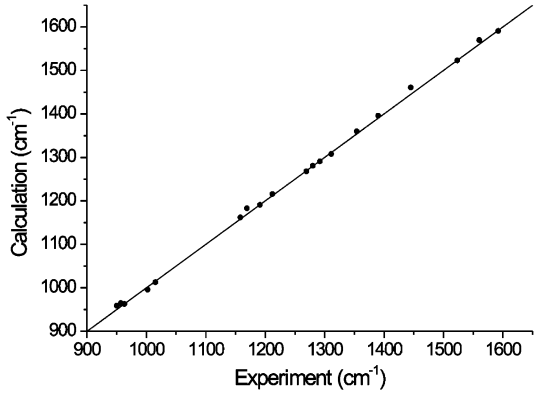

Figure 4. Correlation of experimental and calculated Raman frequencies for *all-trans*-spheroidene. Each experimental frequency is coupled to the closest calculated frequency for which appreciable resonance Raman intensity is predicted.

Table 3), which for NA spheroidene was not experimentally resolved but was recognized already from the larger bandwidth of the 1523 cm^{-1} band.[13] The intensity of the second band may become appreciable as for the 13-^{13}C and 15′-^{13}C isotopomers. In those cases two in-phase C═C combinations show up as illustrated in Figure 7 for 15′-^{13}C spheroidene. The mode at higher frequency is composed of the C═C bonds that carry a methyl group (C_9═C_{10}, C_{13}═C_{14}, $C_{14'}$═$C_{13'}$) and the one at lower frequency of the C═C bonds that do not carry a methyl group (C_7═C_8, C_{11}═C_{12}, C_{15}═$C_{15'}$, $C_{12'}$═$C_{11'}$). A similar doubling is found for the 10-^{2}H, 13-^{13}C, and 14′-^{13}C isotopomers, where in the last two cases the order of the two modes has been reversed.

Fingerprint Region. *1130−1170 cm^{-1}.* Normal modes in this range comprise stretch vibrations of the C−C bonds between C_6 and $C_{10'}$, except for those that carry a methyl group, coupled to in-plane H-bend vibrations along this part of the chain. For NA spheroidene, four modes are calculated in this region, of which the two represented in Figure 6b,c have intensity. Upon isotopic substitution, the composition of the modes varies in a subtle way, which is accompanied by substantial intensity redistributions. For nearly all isotopomers two bands with appreciable intensity are calculated and observed (as separate bands, a band with a shoulder, or a broader band). The data for this region are summarized in Table 3. The simplified picture in Figure 5, where for this region the variation of the intensity-weighted average frequency with isotopic composition is represented, illustrates that the agreement between calculation and experiment is good, although less than in the C═C stretch region. The calculated intensity distribution in several cases deviates from that observed, e.g., for natural-abundance spheroidene, as seen in Figure 3. The intensity mismatch may result from errors in the calculated composition of the modes or in the estimated structural change upon excitation, and, most probably, from the severe approximations underlying eq 1.

1170−1300 cm^{-1}. The normal modes again consist of linear combinations of C−C stretch and in-plane H-bend vibrations, but compared with that of the lower frequency part of the fingerprint region, the weight of the H-bend vibrations has increased and the C−C bonds that carry a methyl group take part as well.

For NA spheroidene a normal mode is calculated at 1191 cm^{-1} (and observed at 1191 cm^{-1}) that is little affected by isotopic substitution in the C_{10} to $C_{11'}$ part of the molecule. The mode concerns a linear combination of the C_4−C_5 and C_8−C_9 stretches, bonds that both carry a methyl group.

The calculations show that many modes in this region are more delocalized than thought previously on the basis of a phenomenological analysis of the changes upon isotopic substitution.[13] This, for example, applies to the modes calculated in the 1205−1220 cm^{-1} region. Interestingly, the calculations indicate for many isotopomers a contribution of the C_{15}═$C_{15'}$

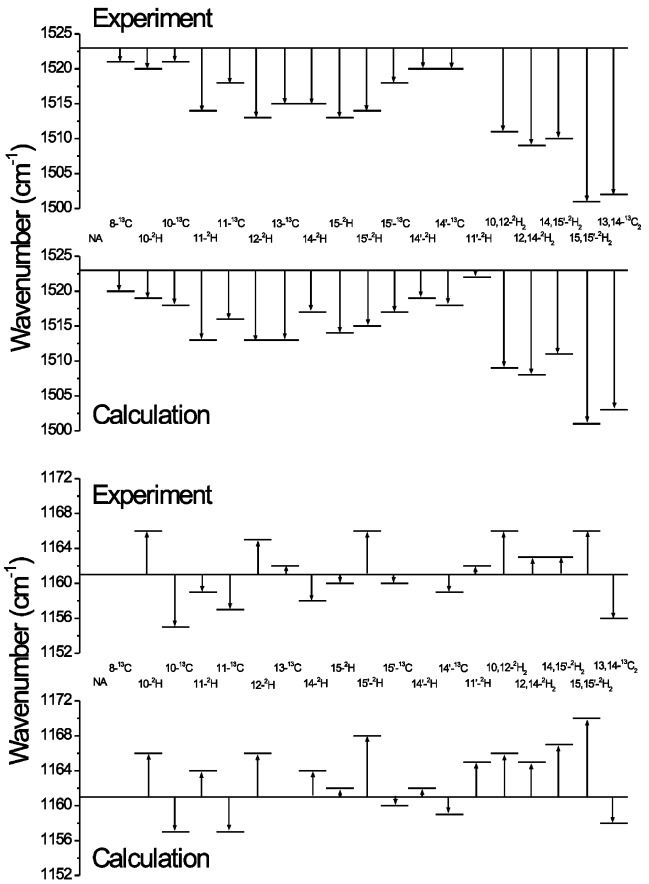

Figure 5. Observed and calculated variation with isotopic substitution of Raman frequencies for *all-trans*-spheroidene relative to NA. Top: the most intense band in the 1500−1600 cm^{-1} region. Bottom: intensity-weighted average frequency of the two most intense bands in the 1130−1170 cm^{-1} region. From left to right: NA, 8-^{13}C, 10-^{2}H, 10-^{13}C, 11-^{2}H, 11-^{13}C, 12-^{2}H, 13-^{13}C, 14-^{2}H, 15-^{2}H, 15′-^{2}H, 15′-^{13}C, 14′-^{2}H, 14′-^{13}C, 11′-^{2}H, 10,12-^{2}H$_2$, 12,14-^{2}H$_2$, 14,15′-^{2}H$_2$, 15,15′-^{2}H$_2$, and 13,14-^{13}C$_2$.

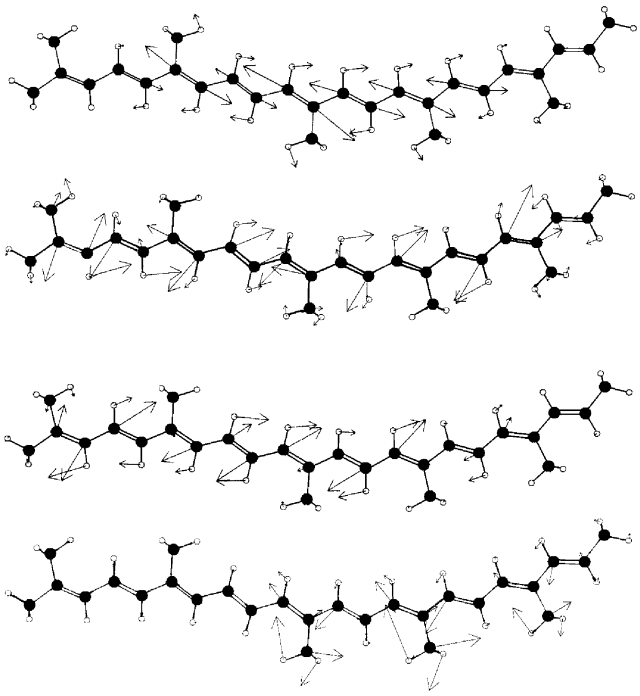

Figure 6. Representation of some calculated normal modes for NA *all-trans*-spheroidene. From top to bottom: (a) 1523 cm^{-1}, (b) 1157 cm^{-1}, (c) 1162 cm^{-1}, and (d) 996 cm^{-1}. The vectors indicate the direction and the relative amplitude of the Cartesian atomic displacements of the normal mode. The amplitudes of the hydrogen displacements have been downscaled by a factor 4 relative to the amplitudes of the carbon displacements.

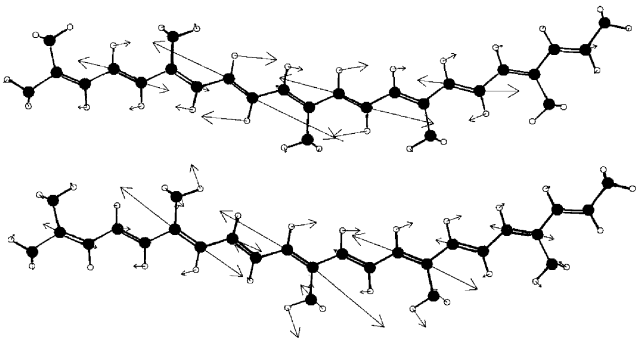

Figure 7. Representation of two calculated normal modes for 15′-^{13}C *all-trans*-spheroidene: (top) 1517 cm^{-1}; (bottom) 1523 cm^{-1}. The vectors indicate the direction and the relative amplitude of the Cartesian atomic displacements of the normal mode. The amplitudes of the hydrogen displacements have been downscaled by a factor 4 relative to the amplitudes of the carbon displacements.

stretch to these modes, which is found to account for, depending on the position of the label, 20−60% of the intensity of such modes.

For NA spheroidene we calculate no normal modes between 1216 and 1256 cm^{-1}, but for several deuterium-labeled isotopomers a relatively localized mode is calculated around 1230 cm^{-1}. The mode structure is schematically represented in Figure 8. Such a motif may be realized for ^{2}H substitution at several positions along the carbon chain, at C_8, C_{12}, C_{15}, and $C_{15'}$ (cf. Figure 1). Indeed, as represented in Table 4, such modes are calculated for the isotopomers containing ^{2}H at these positions, in full agreement with the experimental observations. In addition, the resonance Raman spectra of related doubly ^{2}H-substituted isotopomers sometimes reveal similar bands, for 12,14-$^{2}H_2$ and 15,15′-$^{2}H_2$, and sometimes not, for 10,12-$^{2}H_2$ and 14,15′-$^{2}H_2$. This suggests that a second deuterium replacing the hydrogen that is next to the first deuterium and that undergoes a large amplitude motion in the 1230 cm^{-1} mode of the singly substituted isotopomer prevents the formation of this type of mode in the doubly substituted isotopomer. We then expect such a mode to be present also for 8,*x*-$^{2}H_2$ ($x \neq 6$), 12,*x*-$^{2}H_2$ ($x \neq 10$), 15,*x*-^{2}H2 ($x \neq 14'$), and 15′,*x*-$^{2}H_2$ ($x \neq 14$), which is confirmed by the calculations (cf. Table 4).

The calculations indicate that the occurrence of modes between 1200 and 1220 cm^{-1} and the absence of modes between 1220 and 1240 cm^{-1} (and vice versa) are correlated, which underscores the experimental observation that certain deuterium substitutions seem to shift the 1212 cm^{-1} band for NA spheroidene to the 1220−1240 cm^{-1} region (cf. NA and 15,-15′-$^{2}H_2$ in Figure 3). A related observation concerns the appearance of a band around 1270 cm^{-1} upon substitution of ^{2}H at other positions. Calculations point to a mode with appreciable intensity around this frequency, in agreement with experiment, upon substitution at C_{10}, C_{14}, and $C_{14'}$. Of all ^{2}H-substituted spheroidenes studied experimentally, the only isotopomer that shows no intensity between 1215 and 1300 cm^{-1} concerns 11-^{2}H spheroidene, in full agreement with the results of the calculations.

1002 cm^{-1} Band. The calculations show that this band concerns the in-phase combination of the rock vibrations of the methyl groups at C_5, C_9, and C_{13}. The calculated frequency of this mode is 996 cm^{-1} for NA spheroidene, which is 6 cm^{-1}

TABLE 3: Calculated and Experimental Frequencies for Natural-Abundance and Isotopically Substituted *all-trans*-Spheroidenes in Two Regions of the Resonance Raman Spectrum[a]

	1500−1565 cm^{-1}		1150−1170 cm^{-1}	
isotopomer	calc	exp	calc	exp
NA	1523 (100)	1523 (100)	1157 (6)	1158 (39)
	1530 (8)	(s)	1162 (35)	1169 (12)
8-^{13}C	1520 (100)	1521 (100)	1157 (6)	1160 (63)
	1554 (6)	1551 (9)	1162 (35)	1168 (14)
10-^{13}C	1518 (100)	1521 (100)	1154 (25)	1153 (70)
	1529 (30)	(s)	1160 (23)	1165 (12)
11-^{13}C	1516 (100)	1518 (100)	1154 (24)	1155 (68)
	1527 (10)	1531 (27)	1160 (19)	1165 (12)
13-^{13}C	1513 (100)	1515 (88)	1156 (14)	1160 (100)
	1529 (68)	1530 (56)	1162 (56)	1170 (20)
15′-^{13}C	1517 (100)	1518 (100)	1155 (17)	1155 (66)
	1524 (64)	1528 (89)	1162 (40)	1167 (46)
14′-^{13}C	1518 (100)	1520 (100)	1156 (15)	1155 (34)
	1529 (38)	1530 (45)	1161 (32)	1166 (20)
13,14-$^{13}C_2$	1503 (71)	1502 (50)	1158 (88)	1156 (100)
	1528 (100)	1529 (48)		
10-^{2}H	1519 (100)	1520 (100)	1166 (26)	1166 (21)
	1530 (12)	(s)		
11-^{2}H	1513 (100)	1514 (100)	1156 (6)	1156 (37)
	1528 (4)	1526 (10)	1166 (27)	1162 (49)
12-^{2}H	1513 (100)	1513 (100)	1160 (5)	1159 (35)
	1559 (7)	1557 (7)	1167 (24)	1170 (44)
14-^{2}H	1517 (100)	1515 (100)	1156 (7)	1158 (85)
	1530 (22)	1528 (35)	1166 (32)	
15-^{2}H	1514 (100)	1513 (100)	1157 (6)	1156 (27)
	1527 (5)	1530 (15)	1164 (27)	1163 (39)
15′-^{2}H	1515 (100)	1514 (100)		1163 (34)
	1526 (11)	1529 (18)	1168 (28)	1170 (27)
14′-^{2}H	1519 (100)	1520 (100)	1157 (5)	1158 (57)
	1530 (13)	1530 (11)	1163 (35)	1170 (19)
11′-^{2}H	1522 (100)	1523 (100)	1165 (39)	1162 (63)
10,12-$^{2}H_2$	1509 (100)	1511 (100)	1166 (22)	1162 (20)
				1171 (16)
12,14-$^{2}H_2$	1508 (100)	1509 (100)	1149 (4)	1156 (19)
	1558 (6)	1561 (4)	1168 (24)	1167 (28)
14,15′-$^{2}H_2$	1511 (100)	1510 (100)	1167 (31)	1163 (60)
	1565 (5)	1562 (3)		
15,15′-$^{2}H_2$	1501 (100)	1501 (100)	1157 (3)	1155 (14)
	1526 (25)	1529 (27)	1172 (23)	1172 (29)
	1565 (6)	1560 (4)		

[a] Intensities are given in parentheses, relative to the highest intensity band in the calculated or the experimental spectrum. Calculated bands with an intensity smaller than 3% are not listed. Shoulders in the experimental spectrum are indicated by (s).

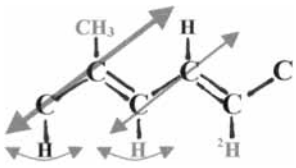

Figure 8. Schematic representation of the composition of the relatively localized normal mode observed for several isotopomers of *all-trans*-spheroidene around 1230 cm^{-1}. The arrows denote the characteristic vibrations. According to our calculations, this type of mode is prevented from formation by deuteration of the ^{1}H atom displayed in gray. Upon deuteration of one of the ^{1}H atoms displayed in black, the motif is retained.

too low. The observed frequency of this mode is virtually unaffected by ^{13}C or ^{2}H substitution, which is reproduced by the calculation: 996 ± 1 cm^{-1} for 16 isotopomers. The only exceptions concern 14-^{2}H and 14,15′-$^{2}H_2$ spheroidene. Experimentally, an upward frequency shift is noticed for these isotopomers. The calculations also reveal such a shift and indicate a 5-fold reduction in intensity of this mode upon ^{2}H substitution at the C_{14} position. The mode composition for NA spheroidene is represented in Figure 6d. The C_{13}−CH_3 rock is coupled to the 14-H in-plane bend and to the out-of-phase combination of the C_{13}=C_{14} and C_{12}−C_{13} stretch vibrations. Substitution of ^{2}H at C_{14} removes the coupling, also to the stretches whose participation accounts for the intensity.

TABLE 4: Calculated Frequencies and Intensities of Modes around 1230 cm^{-1} for Some Isotopomers of *all-trans*-Spheroidene[a]

isotopomer	exp freq (cm^{-1})	calc freq (cm^{-1})	calc int (au)
12-^{2}H	1232	1233	0.26
15-^{2}H	1234	1232	0.22
15′-^{2}H	1238	1238	0.11
12,14-$^{2}H_2$	1229	1230	0.11
15,15′-$^{2}H_2$	1229	1228	0.25
		1236	0.02
8-^{2}H		1227	0.04
7,8-$^{2}H_2$		1223	0.09
4,8-$^{2}H_2$		1236	0.08
8,10-$^{2}H_2$		1222	0.03
8,12-$^{2}H_2$		1221	0.03
		1241	0.32
10,15-$^{2}H_2$		1232	0.23
11,12-$^{2}H_2$		1233	0.18
15,12′-$^{2}H_2$		1243	0.30

[a] For those isotopomers considered experimentally, the observed frequencies are listed as well.

950 cm^{-1} Region. For the ^{2}H-isotopomers invariably a band having appreciable resonance Raman intensity is calculated (and observed) around 950 cm^{-1} (cf. 15,15′-$^{2}H_2$ in Figure 3). This band corresponds to an in-plane deuterium bend vibration, which under the substitution of ^{1}H for ^{2}H shifts to lower frequency and largely decouples from the C−C stretch and ^{1}H-bend vibrations.

Recently, after completion of the present work, a paper by Mukai-Kuroda et al.[23] appeared that describes the analysis of the resonance Raman spectra of natural-abundance *all-trans*-spheroidene and 7 ^{2}H-containing isotopomers based on an empirical normal-coordinate analysis. Their results deviate significantly from those presented here and seem to be at variance with the structure of the conjugated part of the spheroidene molecule. In particular, in contrast to our calculation (cf. Table 2), the normal modes are found to be symmetric around the C_{15}=$C_{15'}$ bond and rather localized. Both experimental and theoretical aspects seem to be at the basis of the differences. The experimental spectra of Mukai-Kuroda et al. deviate from ours in two respects. First, the absolute frequencies of many Raman bands differ, e.g., 1529 cm^{-1} for their most intense band in the NA spectrum and 1523 cm^{-1} for ours. These differences most probably result from inaccurate calibration for which Mukai-Kuroda et al. used solvent lines instead of atomic lines. The deviations are of the order of the shifts observed upon ^{2}H substitution and therefore have a significant effect on the interpretation. Second, the experimental spectra of Mukai-Kuroda et al. are less resolved. With regard to the theoretical aspects, in their normal-coordinate analysis Mukai-Kuroda et al. assume bond lengths and bond angles estimated on the basis of the X-ray structure of β-carotene (a carotenoid symmetric around C_{15}=$C_{15'}$, in contrast to spheroidene, cf. Figure 1), and this structure differs largely from our optimized geometry (Tables 1 and 1S). In addition, to establish a force field, Mukai-Kuroda et al. used the frequencies of 71 Raman lines to fit 57 force constants. Previous attempts on our side along these lines were unsuccessful although we made use of the Raman spectra of NA and even 10 ^{2}H- or ^{13}C-substituted *all-trans*-spheroidenes.[24] In our opinion, a description based on a semiempirical

force field contains, for a molecule of the size of (the conjugated part of) spheroidene, too many parameters to enable a unique optimization.

Conclusion

The resonance Raman spectrum of *all-trans*-spheroidene has been analyzed on the basis of a DFT calculation. Besides the spectrum of natural-abundance spheroidene, the spectra of 19 ^{2}H- or ^{13}C-labeled isotopomers were taken into consideration. The variations in the observed spectrum upon isotopic substitution are nicely reproduced, from which we conclude that the theoretical method to calculate the normal modes works even for a large molecule like a carotenoid. This result sets the stage for the study of the 15,15′-*cis*-spheroidene in the reaction center of *Rh. sphaeroides*. In this case we also have at our disposal the resonance Raman spectra of NA spheroidene and many isotopomers but the structure is largely unknown. The challenge is to find the structure whose calculated resonance Raman spectra for all isotopomers reproduce the experimental data. Calculations presently underway show that such an approach is feasible.

Acknowledgment. This work has been performed under the auspices of the BIOMAC Research School of the Leiden and Delft Universities and was supported with financial aid by The Netherlands Organisation for Scientific Research (NWO), department of Chemical Sciences (CW). The work in the laboratory of H.A.F. was supported by a grant from the National Institutes of Health (GM-30353).

Supporting Information Available: (i) The fully optimized structure of *all-trans*-spheroidene. (ii) All calculated normal-mode frequencies and resonance Raman intensities for all isotopomers. This material is available free of charge via the Internet at http://pubs.acs.org.

References and Notes

(1) Rauhut, G.; Pulay, P. *J. Phys. Chem.* **1995**, *99*, 3093−3100.
(2) Scott, A. P.; Radom, L. *J. Phys. Chem.* **1996**, *100*, 16502−16513.
(3) Wong, M. W. *Chem. Phys. Lett.* **1996**, *256*, 391−399.
(4) Schettino, V.; Gervasio, F. L.; Cardini, G.; Salvi, P. R. *J. Chem. Phys.* **1999**, *110*, 3241−3250.
(5) In ‘t Velt, C. M.; van Hemert, M. C.; Groenen, E. J. J. Unpublished results.
(6) Schettino, V.; Salvi, P. R.; Bini, R.; Cardini, G. *J. Chem. Phys.* **1994**, *101*, 11079−11081.
(7) Cogdell, R. J.; Parson, W. W.; Kerr, M. A. *Biochim. Biophys. Acta* **1976**, *430*, 83−93.
(8) Lutz, M.; Szponarski, W.; Berger, G.; Robert, B.; Neumann, J. *Biochim. Biophys. Acta* **1987**, *894*, 423−433.
(9) de Groot, H. J. M.; Gebhard, R.; van der Hoef, K.; Hoff, A. J.; Lugtenburg, J.; Violette, C. A.; Frank, H. A. *Biochemistry* **1992**, *31*, 12446−12450.
(10) Yeates, T. O.; Komiya, H.; Chirino, A.; Rees, D. C.; Allen, J. P.; Feher, G. *Proc. Natl. Acad. Sci. U.S.A.* **1988**, *85*, 7993−7997. Arnoux, B.; Ducruix, A.; Reiss-Husson, F.; Lutz, M.; Norris, J.; Schiffer, M.; Chang, C.-H. *FEBS Lett.* **1989**, *258*, 47−50. Ermler, U.; Fritzsch, G.; Buchanan, S. K.; Michel, H. *Structure* **1994**, *2*, 925−936.
(11) McAuley, K. E.; Fyfe, P. K.; Ridge, J. P.; Cogdell, R. J.; Isaacs, N. W.; Jones M. R. *Biochemistry* **2000**, *39*, 15032−15043.
(12) Kok, P.; Köhler, J.; Groenen, E. J. J.; Gebhard, R.; van der Hoef, K.; Lugtenburg, J.; Hoff, A. J.; Farhoosh, R.; Frank, H. A. *Biochim. Biophys. Acta* **1994**, *1185*, 188−192.
(13) Kok, P.; Köhler, J.; Groenen, E. J. J.; Gebhard, R.; van der Hoef, K.; Lugtenburg, J.; Farhoosh, R.; Frank, H. A. *Spectrochim. Acta* **1997**, *A53*, 381−392.
(14) Frisch, M. J.; Trucks, G. W.; Schlegel, H. B.; Scuseria, G. E.; Robb, M. A.; Cheeseman, J. R.; Zakrzewski, V. G.; Montgomery, J. A., Jr.; Stratmann, R. E.; Burant, J. C.; Dapprich, S.; Millam, J. M.; Daniels, A. D.; Kudin, K. N.; Strain, M. C.; Farkas, O.; Tomasi, J.; Barone, V.; Cossi, M.; Cammi, R.; Mennucci, B.; Pomelli, C.; Adamo, C.; Clifford, S.; Ochterski, J.; Petersson, G. A.; Ayala, P. Y.; Cui, Q.; Morokuma, K.; Malick, D. K.; Rabuck, A. D.; Raghavachari, K.; Foresman, J. B.; Cioslowski, J.; Ortiz, J. V.; Stefanov, B. B.; Liu, G.; Liashenko, A.; Piskorz, P.; Komaromi, I.; Gomperts, R.; Martin, R. L.; Fox, D. J.; Keith, T.; Al-Laham, M. A.; Peng, C. Y.; Nanayakkara, A.; Gonzalez, C.; Challacombe, M.; Gill, P. M. W.; Johnson, B.; Chen, W.; Wong, M. W.; Andres, J. L.; Gonzalez, C.; Head-Gordon, M.; Replogle, E. S.; Pople, J. A. *Gaussian 98*, revision A.5; Gaussian, Inc.: Pittsburgh, PA, 1998.
(15) Connors, R. E.; Burns, D. S.; Farhoosh, R.; Frank, H. A. *J. Phys. Chem.* **1993**, *97*, 9351−9355.
(16) Albrecht, A. C. *J. Chem. Phys.* **1961**, *34*, 1476−1484.
(17) Warshel, A.; Dauber, P. *J. Chem. Phys.* **1977**, *66*, 5477−5488.
(18) Myers, A. B.; Harris, R. A.; Mathies, R. A. *J. Chem. Phys.* **1983**, *79*, 603−613.
(19) Warshel, A.; Karplus, M. *J. Am. Chem. Soc.* **1974**, *96*, 5677−5689.
(20) To be published.
(21) Curry, B.; Palings, I.; Broek, A. D.; Pardoen, J. A.; Lugtenburg, J.; Mathies, R. *Adv. Infrared Raman Spectrosc.* **1985**, *12*, 115−178.
(22) Koyama, Y.; Takatsuka, I.; Nakata, M.; Tasumi, M. *J. Raman Spectrosc.* **1988**, *19*, 37−49.
(23) Mukai-Kuroda, Y.; Fujii, R.; Ko-chi, N.; Sashima, T.; Koyama, Y.; Abe, M.; Gebhard, R.; Van der Hoef, I.; Lugtenburg, J. *J. Phys. Chem. A* **2002**, *106*, 3566−3579.
(24) Kok, P. Ph.D. Thesis, Leiden University, 1996.